Babylonian Journal of Mathematics
Vol. **2025, pp**. 1–11
DOI:https://doi.org/10.58496/BJM/2025/001; ISSN:3006-113X
https://mesopotamian.press/journals/index.php/mathematics

Research Article

Chemical Reaction and Activation Energy Impacts on Unsteady Radiative Flow of Sisko Fluid

Wahid Rehman [1,*], Fabio Souto De Azevedo [1], Shakir Ullah [2]

[1] *Department of Mathematics, Universidade Federal do Rio Grande do Sul Campus Do Vale, Brazil*.

[2] *Department of Physics, Government Post Graduate College, Karak KP, 27200, Pakistan*.

ARTICLEINFO

Article History

Received 21 Oct 2024
Revised: 20 Nov 2024
Accepted 18 Dec 2024
Published 19 Jan 2025

Keywords

Sisko fluid

Unsteady Radiative Flow,

Activation Energy
Stretching surface

ABSTRACT

In this work, we study the two-dimensional boundary layer flow of Sisko fluid over stretching surface. Further we have observed, the effect of chemical reaction and activation energy on unsteady radiative flow of Sisko fluid. The suitable transformations are used to convert non-linear partial differential equations (PDEs) into ordinary differential equations (ODEs). Numerical solutions are obtained for the velocity, temperature and concentration profiles by utilizing the bvp4c technique. The effect of various parameters on the heat transfer and concentration profiles are depicted in the graphs and tables are briefly discussed.

1. INTRODUCTION

Due to boundary layer flow has several applications in technology and engineering, it is significant when it occurs across a stretched surface. Such a sheet creates movement in fluid when surfaces inflate or contract, like when bubbles and pseudopods elongate. In particular, stretching flow happens in the cooling bath, during paper chilling and drawing, during textile and glass fiber manufacture, etc. In these instances, the ultimate outcome of these attributes is contingent upon the pace of stretching, the rate of cooling throughout the entire process, and the stretching mechanism itself. The investigation of boundary layer flow across a continuous, uniformly-moving solid surface was first carried out by Sakiadis [1]. Later, Crane [2] investigated the boundary flow of Newtonian fluid resulting from the stretching of an elastic at sheet that travels in its own plane under uniform stress, with a velocity that varies linearly with distance from a fixed point. The micropolar fluid flow via a stretched sheet with a changing surface temperature was examined by Hassanien et al. [3].

The effect of a uniform magnetic field on the flow of an electrically conducting Visco-elastic fluid across a stretched sheet was investigated by Anderson et al. [4]. The MHD flow of an electrically conducting power law fluid across a stretched surface in the presence of a transverse magnetic field was also studied by Andersson [5]. There has been a great deal of research on boundary layer flow across stretched surfaces [6-10].

In the field of fluid mechanics, the Rayleigh dilemma and the Stokes oscillating plate are typical manifestations of unsteady boundary layers. Unsteady boundary layers differ from steady state in that they are caused by an additional time-dependent term that is included in the governing equations and can influence fluid structure, movement, and boundary layer separation [11, 12]. A non-uniform source of heat and an unstable stretching surface were the subjects of a study by Tsai et al. [13]. Todd [14] developed a significant unstable boundary layer problem for a free stream flowing at a constant velocity across an established semi-infinite flat plate. This also included a detailed discussion of the momentum boundary layer and an evolving leading edge including a flow with a particular rate of accretion or ablation. Unsteady stretching flow problems have received a lot of interest lately; some of them are discussed in [15-17]. The problem of heat transmission across an unstable stretched surface with a predetermined wall temperature has been studied by Ishak et al. [18]. The impact of

*Corresponding author. Email: Wahid Rehman@gmail.com

changing fluid characteristics on the MHD flow and heat transfer of Ostwald-de Waele fluid across an unstable stretched sheet was investigated by Vajravelu et al. [19]. The unsteady flow and heat transport in a power law fluid across an unstable radially extending surface were studied by Ahmed et al. [20].

The practical significance of magnetohydrodynamics in engineering has grown in importance. This kind of flow can be employed to address issues with induction flow meters, which rely only on the fluid s potential difference orthogonal to the direction of motion and the magnetic field. The unstable hydro-magnetic flow as well as heat transfer from a non-isothermal stretched sheet submerged in a porous medium were examined by Chamkha [21]. A comparable non-linear problem was solved by Liao [22] using HAM. The MHD flow in the Jaffrey fluid model over a stretched sheet with radiative heat transfer was examined by Ahmed et al. [23]. There was a noticeable drop as the magnetic field strength increased. An external magnetic field has been the subject of much research, as evidenced by the literature [24, 25]. Applications for ow via suction or injection in engineering include gaseous diffusion, environmental contamination, and rotational particle separation [26].

As far as we are aware, there has not yet been any attempt to use the activation energy and concentration idea to simulate the flow of the Sisko fluid model across an unstable stretching surface. This gap is being filled by the current investigation. Pseudoplastic and dilatant fluid behavior may be predicted by the Sisko fluid model. The Sisko model applies to many actual fluids. The field of oil engineering regularly use this paradigm. For the movement of greases, the Sisko fluid model is the most appropriate [27]. Not much research has been done with this model, considering its wide range of usage in industry [28, 29].

The current study examines the heat transmission and MHD flow of a Sisko fluid across an unstable planner stretchable surface using suction. By employing reasonable similarity transformations, the nonlinear partial differential equations (PDEs) are reduced to ordinary differential equations (ODEs). We use the bvp4c approach for numerical solutions. A detailed discussion is also given to the impacts on the temperature, velocity, and concentration profiles for different factors.

2. FLOW GOVERNING EQUATIONS

Let us consider unsteady, two-dimensional boundary layer flow of in-compressible over a stretching sheet in the presence of melting with non-linear thermal radiation and concentration equation. Time dependent uniform magnetic field perpendicularly applied to sheet. By the assumptions of weak magnetic field due to by which magnetic induction phenomenon effect vanishes. More-ever the velocity component u and v are along x- and y- direction respectively. The flow is caused by unsteady stretched of the sheet along x-axis. The following equations governed are used for the above assumptions

$$\frac{\partial u}{\partial x}+\frac{\partial v}{\partial y}=0, \tag{1}$$

$$\frac{\partial u}{\partial t}+u\frac{\partial u}{\partial x}+v\frac{\partial u}{\partial y}=\frac{a}{\rho}\frac{\partial^{2} u}{\partial y^{2}}-\frac{\partial}{\partial y}\left[\frac{-\partial u}{\partial y}\right]^{n}-\left(\frac{\sigma B^{2}}{\rho}\right)u, \tag{2}$$

$$\frac{\partial T}{\partial t}+u\frac{\partial T}{\partial x}+v\frac{\partial T}{\partial y}=\alpha\frac{\partial^{2} T}{\partial y^{2}}-\frac{1}{\rho c_{p}}\frac{\partial}{\partial y}\left(\frac{-4\sigma^{*}}{3k^{*}}\frac{\partial T^{4}}{\partial y}\right),7 \tag{3}$$

$$\frac{\partial C}{\partial t}+u\frac{\partial C}{\partial x}+v\frac{\partial C}{\partial y}=\frac{D}{\rho c}\frac{\partial^{2} C}{\partial y^{2}}-K_{r}^{2}(C-C_{\infty})\left(\frac{T}{T_{\infty}}\right)^{n}\exp^{\frac{-Ea}{KT}}. \tag{4}$$

The relevant boundary conditions are:

$$u=U_{w}=\frac{cx}{1-\alpha t}, v=-f(x,t)=v_{w}, T=T_{w}, C=C_{w} aty=0, \tag{5}$$

$$u=0, T\longrightarrow\infty, C\longrightarrow\infty \text{ as } y\longrightarrow\infty. \tag{6}$$

In the above expression u and v are the components of velocity along x and y direction respectively, n is the power law index with a and b are material constants, T is the temperature, the thermal diffusivity, k is the thermal conductivity and c_p is the specific heat, where q_r is radiative heat flux in equation is given by Rosseland approximation as follows

$$q_{r}=\frac{-4\sigma^{*}}{3k^{*}}\frac{\partial T^{4}}{\partial y} \tag{7}$$

where σ^{*} the Stefan-Boltzmann constant and k^{*} the mean absorption coefficient. We introduce the following similarity transformations

$$\Psi(x,y)=\frac{cx}{1-\alpha t}\left(x(\Re_b)^{\frac{-1}{1+n}}f(\eta)\right);\qquad \eta=\frac{y}{x}(\Re_b)^{\frac{1}{1+n}} \tag{8}$$

$$\phi(\eta)=\frac{C-C_\infty}{c_\infty};\qquad (\eta)=\frac{T-T_\infty}{T_s-T_\infty}. \tag{9}$$

Here (*x; y*) denotes the stream-function in standard form we can write as

$$u=\frac{\partial\psi}{\partial y},v=\frac{-\partial\psi}{\partial x}, \tag{10}$$

which undoubted fulfill the continuity equation, is the similarity variable $f(\eta)$ being the similarity function, $\theta(\eta)$ is the dimensionless temperature $\phi(\eta)$ is the dimensionless volume fraction. By using these similarity variables, the non-dimensional form of the governing equations is stated below as

$$A^*f'''+n(-f'')^{\frac{1}{1+n}}+\frac{2n}{1+n}f''f-f'^2-Mf'-A\left(\left(\frac{2-n}{1+n}\right)\eta f''+f'\right)=0 \tag{11}$$

$$[(1+Rd(1+(\theta_w-1))\theta^3)\theta']'-Prf'\theta+\left(\frac{2n}{1+n}\right)Prf\theta'-APr.\theta+APr\left(\frac{2-n}{1+n}\right)\eta\theta=0, \tag{12}$$

$$\varphi''+Sc\frac{2n}{1+n}f\phi'-Scf'\theta-ASc\left[\phi+\left(\frac{2-n}{1+n}\right)\eta\phi'\right]-Sc.\sigma(1+\sigma\theta)^n.\phi.\exp^{\frac{-E}{1+\sigma\theta}}=0. \tag{13}$$

The non-dimensional boundary condition is

$$f(0)=S,f'(0)=1,f'(\infty)=0,\theta(0)=1,\theta'(\infty)=0,\phi(0)=1,\phi'(\infty)=0. \tag{14}$$

In the above equations, prime indicates differentiation with references to η. In this equations S is the mass transfer parameter. Now in a case of mass suction, we select $S > 0$ and for injection, the criteria are in that form $S < 0$. The other parameters in the above equation are defined as

$$A^*=\frac{\Re_b^{\frac{-2}{1+n}}}{\Re_a},A=\frac{\alpha}{c},M=B_o^2\frac{\sigma}{c_p},Pr=x\frac{\frac{cx}{1-\alpha t}}{\alpha}\Re_b^{\frac{-2}{1+n}},E=\frac{\varepsilon a}{KT_\infty}, \tag{15}$$

$$\sigma=\frac{kr^2}{c},\theta_w=\frac{T_s}{T_\infty},Sc=\frac{v}{D}. \tag{16}$$

3. PARAMETERS OF PHYSICAL INTEREST

In this problem the main term, that we will use is the local skin friction that can be defined as

$$C_f=\frac{\tau_w}{1/2\,U^2\rho},\tau_w=a+b.\left|\frac{\partial u}{\partial y}\right|^{n-1}\frac{\partial u}{\partial y}\Big|_{y=0}=0. \tag{17}$$

and the dimensionless variable can be the form

$$A^*f''(0)-(-1)^n\big(f''(0)\big)^n=\frac{1}{2}C_f\Re_b^{\frac{-1}{1+n}}. \tag{18}$$

The local Nusselt number Nu_x at the wall can be defined as:

$$Nu_x=\frac{xq_w}{T_s-T_\infty}. \tag{19}$$

where the term q_w that is mention in the above heat flux its mathematics can be written as

$$q_w=\left(\frac{\delta T}{\delta y}\Big|_{y=0}\right)(k)=0, \tag{20}$$

which reduces to

$$Nu_x(\Re_b)^{\frac{1}{1+n}}=-\theta'(0). \tag{21}$$

4. SOLUTION METHODOLOGY

Numerical approach is used to find the solution of nonlinear differential equations with the boundary conditions specified in Eqs. (11), (12), (13), and (14). The nonlinear differential equations with power law index (n) are solved using the bvp4c technique. The nonlinear differential equation will first be changed into a system of seven first-order ordinary differential equations, as shown below

$$f = y_1, f' = y_2, f'' = y_3, f''' = y'_3, \tag{22}$$

$$\theta = y_4, \theta' = y_5, \theta'' = y'_5, \tag{23}$$

$$\phi = y_6, \phi' = y_7, \phi'' = y'_7. \tag{24}$$

In contrast to Eqs. (22) (24) which only provides four initial conditions, the solution to our seven ODEs can only be reached when we have seven initial conditions. As a result, an appropriate starting approximation for $y_3(0)$, $y_5(0)$ and $y_7(0)$ is chosen; in this case, we suppose that they are -1. The answer is now calculated using the bvp4c approach. If the border residual is smaller than the absolute error tolerance threshold 10^{-6}, the resulting solution will converge. The original estimate will be adjusted using the secant approach until the answer satisfies the desired criteria if the calculated solution does not satisfy the convergence threshold.

5. GRAPHICAL RESULTS AND DISCUSSION

This part of paper contains a variety of findings from the flow and heat transfer of Sisko fluid across a time-dependent stretching surface when a magnetic field is present. The bvp4c approach has been used to numerically solve the nonlinear ordinary differential equations that are subjected to the boundary equations (11), (12), (13), and (14). A detailed analysis and detailed illustrations of the impact of important physical factors on the velocity, temperature, and concentration profiles are provided in Figs. [1] [12].

A brief glance at the velocity profile reveals the physical nature of the boundary layer structure that formed in the vicinity of the sheet. Effect of unsteadiness parameter A on velocity profile are displayed in Figure 1. Figure 1 shows that the velocity profile increases with the increasing value of unsteadiness parameter A for pseudo plastic ($0 < n < 1$) and opposite behavior for dilatant ($n > 1$) fluids.

The effects of magnetic parameter M, on velocity profile are plotted in Figure 2. These figures clearly show that the velocity profile and the thickness of the boundary layer decrease with a rise in the magnetic parameter M for pseudoplastic ($0 < n < 1$) and dilatant ($n > 1$) fluids.

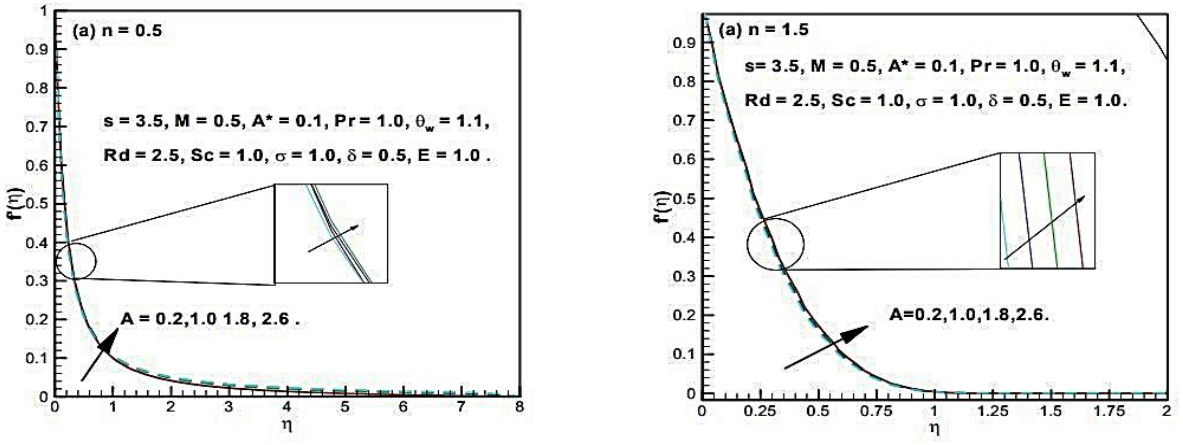

Fig. 1. Fluctuation of velocity profile for distinct values of unsteadiness parameter A for shear thinning and shear thickening fluid.

This suggests that an increment in the magnetic parameter M significantly lowers the rate of transport. It clarifies that the transport phenomenon is opposed by the transverse magnetic field. This is because changes in the magnetic parameter cause changes in the Lorentz force, which in turn provides resistance to the phenomenon of transport. . It clarifies that the transport phenomenon is opposed by the transverse magnetic field. This is because changes in the magnetic parameter cause changes in the Lorentz force, which in turn provides resistance to the phenomenon of transport.

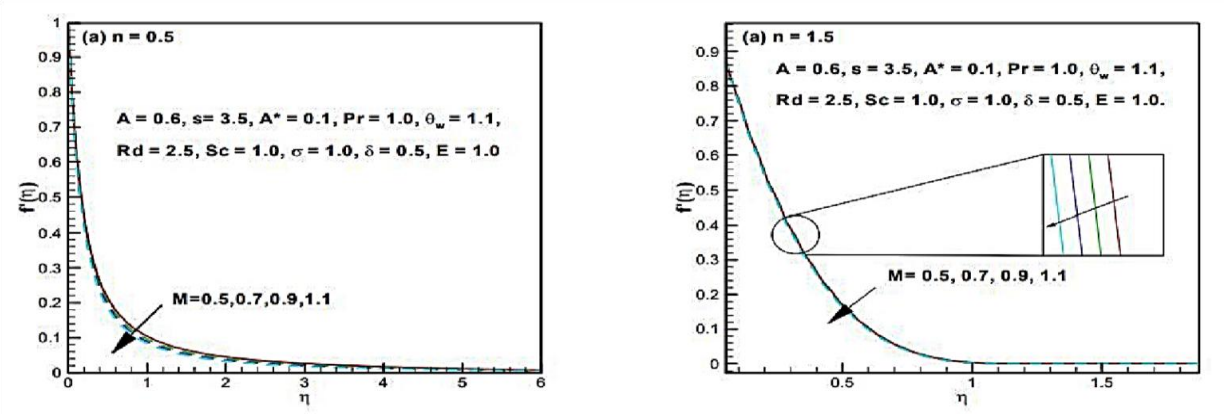

Fig. 2. Fluctuation of velocity pro le for distinct values of magnetic parameter M for shear thinning and shear thickening fluid.

The impact of material parameter A* on the velocity profile is seen in Figure 3. We observed that by increases of A* due to which increment occurs in the boundary layer thickness and velocity profile, for a case of pseudoplastic ($0 < n < 1$) fluid. While opposite effect for dilatant ($n > 1$) fluid.

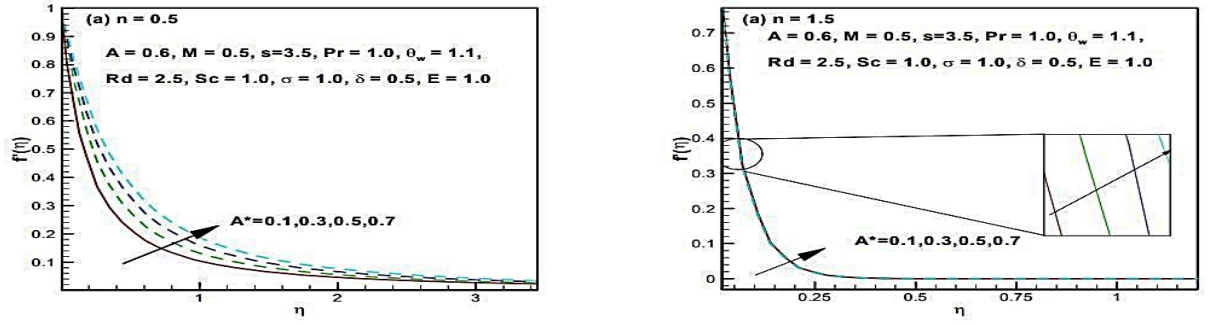

Fig. 3. Fluctuation of velocity profile for distinct values of material parameter A for shear thinning and shear thickening fluid.

Figure 4 is plotted for distinct values of suction parameter *S* for velocity profile. we have seen velocity profile for two types of fluid, i.e., pseudoplastic ($0 < n < 1$) and dilatant ($n > 1$) fluids. These graphs demonstrate how, for all pseudoplastic and dilatant fluids, the suction ($S > 0$) operates to enhance the fluid s adherence to the surface, delaying flow and resulting in a drop in velocity and boundary layer thickness.

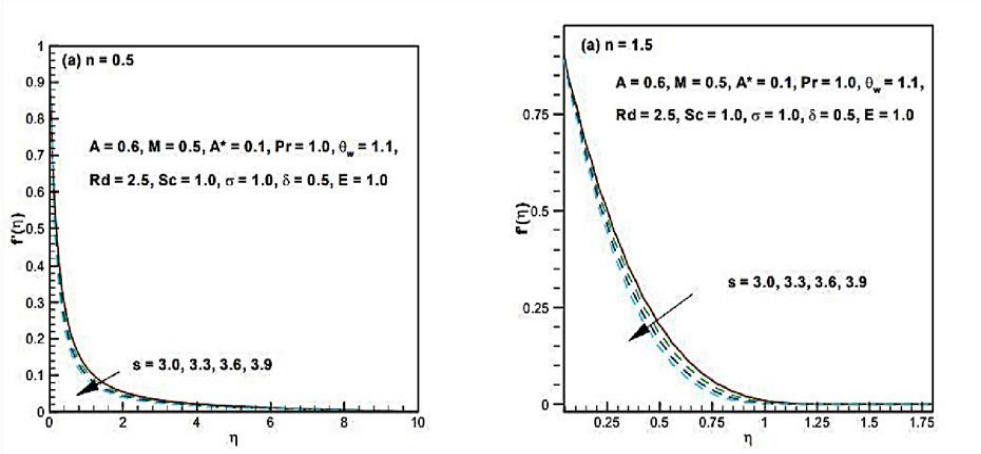

Fig. 4. Fluctuation of velocity profile for distinct values of suction parameter S for shear thinning and shear thickening fluid.

A quick look at the temperature profile will reveal the structure of the thermal boundary layer. Figure 5 represents the temperature profile (η) for distinct values of Prandtl parameter Pr*:* These figures show that the temperature profile (η) decreases with the increasing value of Prandtl parameter Pr for pseudoplastic ($0 < n < 1$) and dilatant ($n > 1$) Fluids.

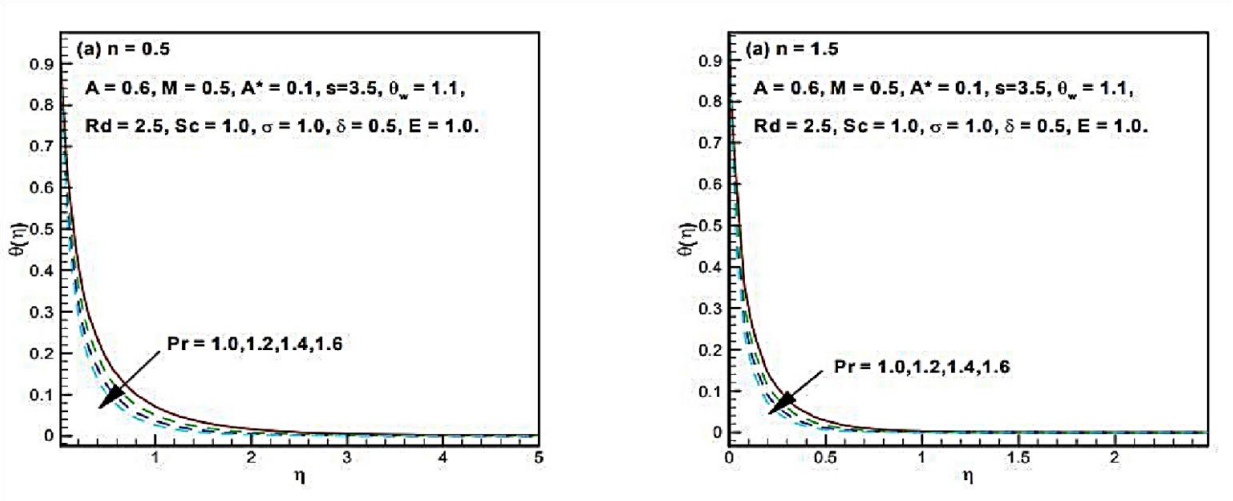

Fig. 5. Fluctuation of temperature profile for distinct values of Prandtl parameter Pr for shear thinning and shear thickening fluid.

The effects of temperature ratio parameter θ_w on temperature profile $\chi(\eta)$ is shown in figure 6. These figures show the temperature profile $q_w = (\frac{\partial T}{\partial y})(k)y = 0(\eta)$ increases with the increasing value of temperature ratio parameter $Nu_x = \frac{xq_w}{T_S - T_\infty}$ for both cases.

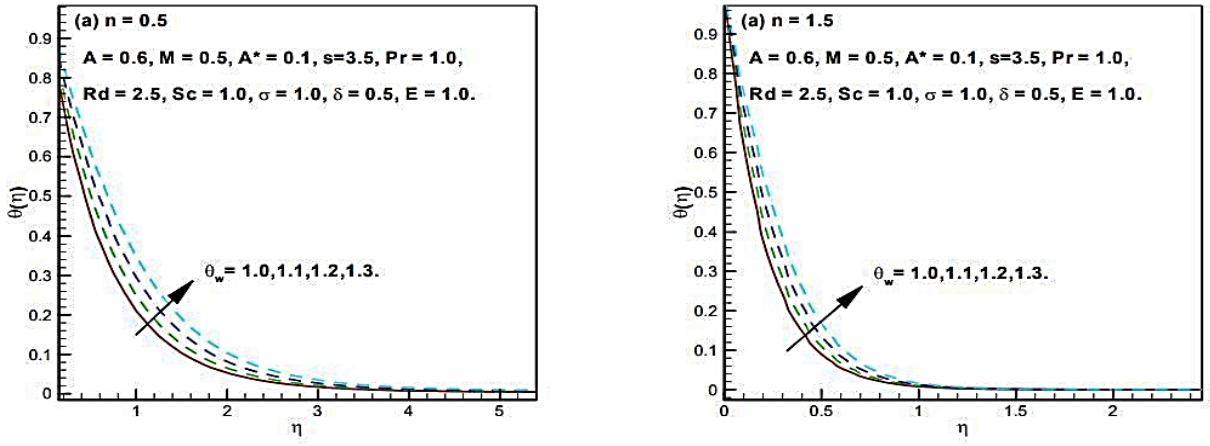

Fig. 6. Fluctuation of temperature profile for distinct values of temperature ratio parameter for shear thinning and shear thickening fluid.

Figure 7 is plotted for temperature profile (η) for distinct values of radiation parameter *Rd*. In both cases increment occurs in boundary layer thickness and temperature profile.

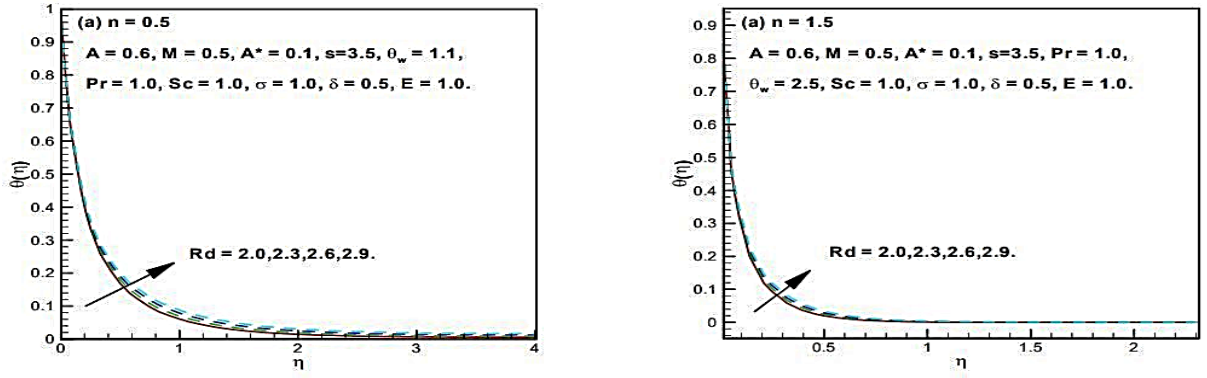

Fig. 7. Fluctuation of temperature profile for distinct values of radiation parameter *Rd* for shear thinning and shear thickening fluid.

Figure 8 illustrates the impact of the unsteadiness parameter A on the temperature profile. It is shown that for pseudoplastic ($0 < n < 1$) and dilatant ($n > 1$) fluid, the thermal boundary layer thickness decreases with an increase in the unsteadiness parameter A.

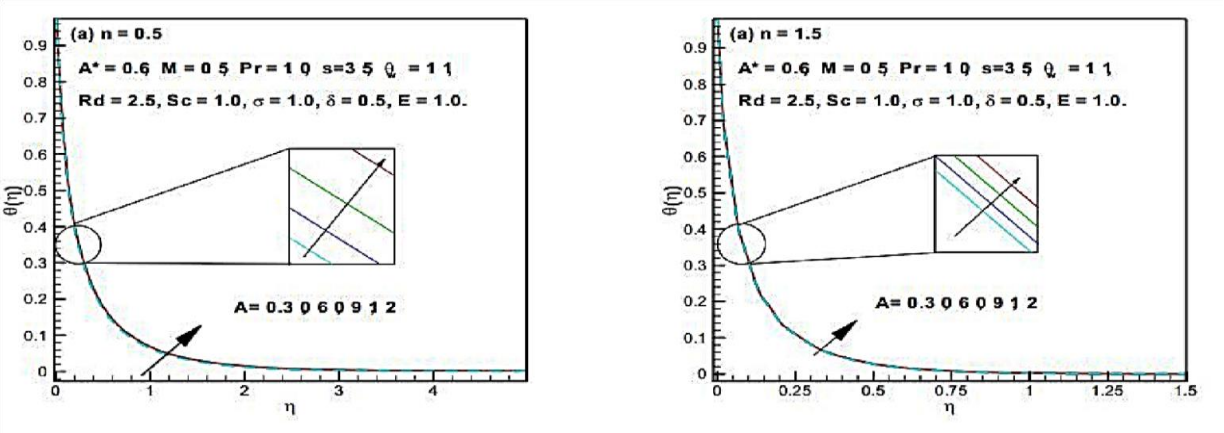

Fig. 8. Fluctuation of temperature profile for distinct values of unsteady parameter A for shear thinning and shear thickening fluid.

We have observed the effects of Schmidt number Sc that have in figure 9. From this figure 9, we see that an increment in Sc causes a decrease in the concentration profile, in a case of pseudoplastic ($0 < n < 1$) and dilatant ($n > 1$) fluids.

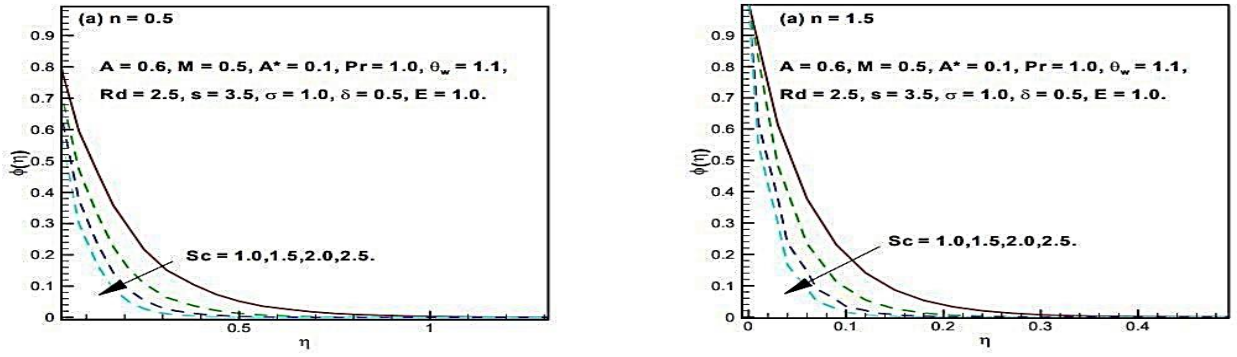

Fig. 9. Fluctuation of concentration profile for distinct values of Schmidth parameter Sc for shear thinning and shear thickening fluid.

In Figure 10, we observed the effect of parameter σ on concentration profile. It is noted that by the increasing values of parameter σ decreases occurs in the concentration profile for pseudoplastic ($0 < n < 1$) and dilatant ($n > 1$) fluids.

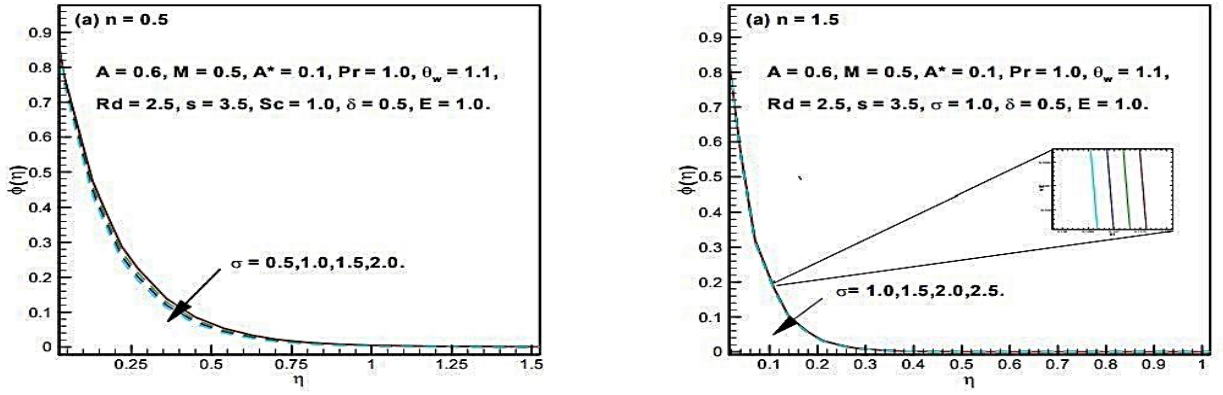

Fig. 10. Fluctuation of concentration profile for distinct values of for shear thinning and shear thickening fluid.

Figure 11 shows the effect of parameter E on concentration profile. By the increasing values of E also increasing occurs in the concentration profile for pseudoplastic ($0 < n < 1$) and dilatant ($n > 1$) Fluids.

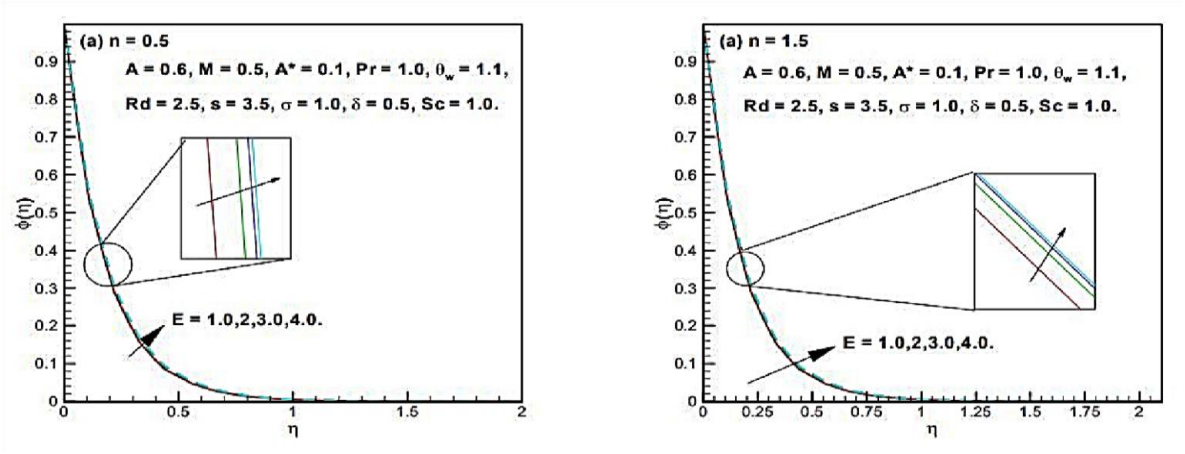

Fig. 11. Fluctuation of concentration profile for distinct values of activation energy E for shear thinning and shear thickening fluid.

Figure 12 shows the effect of parameter δ on concentration profile. It is noted that by increasing values of parameter δ a decrease occurs for pseudoplastic ($0 < n < 1$) and dilatant ($n > 1$) fluids.

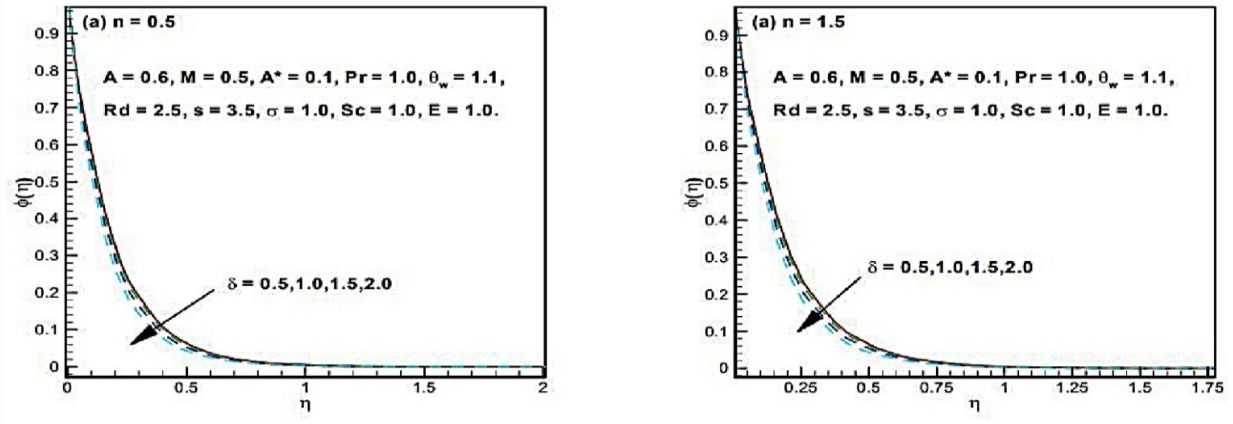

Fig. 12. Fluctuation of concentration profile for distinct values of for shear thinning and shear thickening fluid.

Influence of different physical parameters of interest on the local Skin friction co-efficient C_f is tabulated in Table 1.

TABLE I. NUMERICAL VALUES OF THE LOCAL SKIN FRICTION CO-EFFICIENT FOR DIFFERENT VALUES OF PHYSICAL PARAMETER

				$\frac{1}{2}(\Re_b)^{\frac{1}{1+n}} Cf_x$	
A	***M***	***A***	***s***	***n* = 0.5**	***n* = 1.5**
0.20	0.10	0.20	3.0	2.483000	4.092000
0.40				2.505000	4.141000
0.60				2.530000	4.190000
0.80				2.556000	4.239000
0.20	0.30			2.561000	4.153000
	0.50			2.631000	4.213000
	0.70			2.695000	4.272000
	0.10	0.30		2.532000	4.114000
		0.40		2.579000	4.136000
		0.50		2.623000	4.158000
		0.20	3.20	2.623000	4.314000
			3.40	2.694000	4.538000
			3.60	2.803000	4.762000

From this table it is noted that with an increment in the unsteadiness parameter A, the suction parameter S, the magnetic parameter M and material parameter A the magnitude of the skin friction co-efficient increases for all pseudoplastic ($0 < n < 1$) and dilatant ($n > 1$) fluids.
From table 1, we have observed that with an increase the unsteadiness parameter A, the suction parameter S the magnetic parameter M, material parameter A and Prandtl number the magnitude of the local Nusselt number increases for all pseudoplastic ($0 < n < 1$) and dilatant ($n > 1$) fluids.

TABLE II. NUMERICAL VALUES OF THE LOCAL NUSSELT NUMBER FOR DIFFERENT VALUES OF PHYSICAL PARAMETER

					$-\theta_w$	
A	M	A^*	s	Pr	$n = 0.5$	$n = 1.5$
0.20	0.10	0.20	0.2	1.0	1.040000	1.299000
0.40					1.091000	1.347000
0.60					1.114000	1.394000
0.80					1.197000	1.440000
0.20	0.30				1.013000	1.289000
	0.50				1.990200	1.281000
	0.70				0.969400	1.273000
	0.10	0.30			1.051000	1.313000
		0.40			1.060000	1.323000
		0.50			1.069000	1.332000
		0.20	0.40		1.103000	1.132000
			0.60		1.170000	1.123000
			0.80		1.241000	1.113000
			0.20	1.2	1.165000	1.440000
				1.4	1.283000	1.571000
				1.6	1.394000	1.694000
				1.8	1.50000	1.812000

From table 3. we have noted that with an increase the unsteadiness parameter A, the suction parameter S the magnetic parameter M, material parameter A Schmidt number the magnitude of the local Schmidt number increases for all pseudoplastic ($0 < n < 1$) and dilatant ($n > 1$) fluids.

TABLE III. NUMERICAL VALUES OF THE LOCAL SKIN FRICTION CO-EFFICIENT FOR DIFFERENT VALUES OF PHYSICAL PARAMETER.

								$-\phi(0)$	
A	***M***	***A****	***s***	***Sc***			***E***	***n* = 0.5**	***n* = 1.5**
0.20	0.10	0.20	0.2	0.5	1.0	1.5	0.5	1.000000	1.161000

				1.0				1.373000	1.153000
				1.5				1.281000	1.115000
				2.0				1.113000	1.183000
				1.0	1.2			1.243000	1.151000
					1.4			1.251200	1.132000
					1.6			1.232000	1.112000
					1.0	1.8		1.512000	1.169000
						2.1		1.069000	1.131000
						2.4		1.331000	1.194000
						1.5	0.8	1.494000	1.118000
							1.1	1.623000	1.112000
							1.4	1.618000	1.112000
							1.7	1.812000	1.112000

6. CONCLUSIONS

This study deals with the melting heat transfer and concentration in Sisko fluid ow in presence on non-linear thermal radiation and activation energy. The bvp4c technique has been used to solve the dimensionless governing equation for velocity, temperature and concentration fields. The following main point of the present study are given below:

1. The temperature profile $\theta(\eta)$ increases for increasing values of unsteadiness parameter A of a Sisko fluid and opposite behavior are found for generalized Prandtl number Pr*:*
2. It is noted that temperature profile $\theta(\eta)$ and boundary layer thickness increases for higher values of temperature ratio θ_w parameter.
3. It is observed that temperature profile $\theta(\eta)$ increases are found for radiation parameter Rd.
4. The concentration profile $\phi(\eta)$ decreases for increasing values sigma parameter of a Sisko fluid.
5. It is noted that concentration profile $\phi(\eta)$ and boundary layer thickness decreases for higher values of Schmidth parameter Sc and opposite effect occurs for parameter E*:*
6. It is noted that concentration profile $\phi(\eta)$ and boundary layer thickness decreases for increasing values.

Conflicts Of Interest

The authors have no conflicts of interest to declare.

Funding

The paper does not receive any financial support from institutions or sponsors

Acknowledgment

The author acknowledges the institution for the intellectual resources and academic guidance that significantly enriched this research.

References

[1] B.C. Sakiadis, Boundary layer behavior on continuous solid surface", AIChEJ, 7 (1961), pp. 26-28
[2] L.J. Crane, Flow past a stretching plate", Z Angew Math Phy, 21 (1970), pp. 645-647.
[3] I.A. Hassanien, R.S.R. Gorla, A.A. Abdullah, Flow and heat transfer in a power law fluid over a non-isothermal stretching sheet", Math Comp Mod, 28 (1998), pp. 105-116.
[4] H.I. Andersson, K.H. Bech, B.S. Dandapat, MHD flow of a power law fluid over a stretching sheet", Int J Nonlinear Mech, 27 (1992), pp. 929-936.
[5] H.I. Andersson, Heat transfer in a liquid on an unsteady stretching surface", Int J Heat Mass Transfer, 43 (2000), pp. 69-74.
[6] N. Sandeep, B.R. Kumar, M.S.J. Kumar, A comparative study of convective heat and mass transfer in non-Newtonian nano fluid ow past a permeable stretching sheet", J Mol Liq, 212 (2015), pp. 585-591.
[7] C.S.K. Raju, N. Sandeep, Unsteady three-dimensional ow of Casson Carreau fluids past a stretching surface", Alex Eng J, 55 (2016), pp. 1115-1126.
[8] P.M. Krishna, N. Sandeep, J.V.R. Reddy, V. Sugunamma, Dual solutions for unsteady ow of Powell-Eyring fluid past an inclined stretching sheet", J Naval Arch Marine Eng, 13 (2016), pp. 89-99.
[9] C.S.K. Raju, N. Sandeep, M.J. Babu, V. Sugunamma, Dual solutions for three-dimensional MHD flow of a nanofluid over a nonlinearly permeable stretching sheet", Alex Eng J, 55 (2016), pp. 151-162.
[10] R. Ali, A. Shahzad, M. Khan, M. Ayub, Analytic and numerical solutions for axisymmetric flow with partial slip", Eng Comput, 32 (2016), pp. 149-154.
[11] H.W. Schwarz, The Rayleigh and Stokes problems with an incompressible non-Newtonian fluid", Appl Sci Res, 13 (1964), pp. 161-186.
[12] W. Tan, T. Masuoka, Stoke's first problem for a second-grade fluid in a porous half space with heated boundary", Int J Nonlinear Mech, 40 (2005), pp. 515-522.
[13] R. Tsai, K.H. Huang, J.S. Huang, Flow and heat transfer over an unsteady stretching surface with non-uniform heat source", Int Commun Heat Mass Transfer, 35 (2008), pp. 1340-1343.
[14] L. Todd, A family of laminar boundary layers along a semi-infinite flat plate", Fluid Dyn Res, 19 (1997), pp. 235-249.
[15] T. Fang, A note on the unsteady boundary layers over a flat plate", Int J Nonlinear Mech, 43(2008), pp. 1007-1011.
[16] A. Shahzad, R. Ali, MHD flow of a non-Newtonian power law fluid over a vertical stretching sheet with the convective boundary condition", Walail J Sci Tech, 10 (2013), pp. 43-56.
[17] M. Sajid, I. Ahmed, T. Hayat, M. Ayub, Series solution for unsteady axisymmetric flow and heat transfer over a radially stretching sheet", Commun Nonlinear Sci Numer Simul, 13 (2008), pp. 2193-2203.
[18] A. Ishak, R. Nazar, I. Pop, Heat transfer over an unsteady stretching permeable surface with prescribed wall temperature", Nonlinear Anal Real World Appl, 10 (2009), pp. 2909-2913.
[19] K. Vajravelu, K.V. Parsaad, P.S. Datti, B.T. Raju, MHD flow and heat transfer of an Ostwaldde Waele fluid over an unsteady stretching surface", Ain Shams Eng J, 5 (2014), pp. 157-167.
[20] J. Ahmed, T. Mahmood, Z. Iqbal, A. Shahzad, R. Ali, Axisymmetric ow and heat transfer over an unsteady stretching sheet in power law fluid", J Mol Liq, 221 (2016), pp. 386-393.
[21] A.J. Chamkha, Unsteady hydromagnetic flow and heat transfer form stretching sheet in porous medium", Int Commun Heat Mass Transfer, 25 (1998), pp. 899-906.
[22] S.J. Liao, A new branch of solutions of boundary layerflows over an impermeable stretching plate", Int J Heat Mass Transfer, 48 (2005), pp. 2529-2539.
[23] J. Ahmed, A. Shahzad, M. Khan, R. Ali, A note on convective heat transfer of an MHD Jeffrey fluid over a stretching sheet", AIP Adv, 5 (2015), p. 117117.
[24] Y. Wang, T. Hayat, N. Ali, M. Oberlack, Magnetohydrodynamic peristaltic motion of a Sisko fluid in asymmetric or a symmetric channel", Physica A, 387 (2008), pp. 347-362.
[25] C. Chen, Effects of magnetic eld and suction/injection on convection heat transfer of non-Newtonian power-law fluids past a power-law stretched sheet with surface heat flux", Int. J. Ther. Sci., 47 (2008), pp. 954-961.
[26] R. Cortell, Flow and heat transfer of a fluid through a porous medium over a stretching surface with internal heat generation/absorption and suction/Injection Fluid Dyn Res, 37 (2005), pp.231-245
[27] A.W. Sisko, The ow of lubricating greases", Ind Chem Res, 50 (1958), pp. 1789-1792.
[28] M. Khan, A. Shahzad, On axisymmetric ow of Sisko fluid over a radially stretching sheet", Int J Nonlinear Mech, 47 (2012), pp. 999-1007.
[29] M. Khan, A. Shahzad, On Boundary-layer flow of a Sisko fluid over a stretching sheet", Quaestiones Mathematicae, 36 (2013), pp. 137-151.